

North Pacific cyclonic and anticyclonic transients in a global warming context: possible consequences for Western North American daily precipitation and temperature extremes

Alice Favre · Alexander Gershunov

Received: 20 November 2007 / Accepted: 21 April 2008 / Published online: 15 May 2008
© Springer-Verlag Berlin Heidelberg 2008

Abstract Trajectories of surface cyclones and anticyclones were constructed using an automated scheme by tracking local minima and maxima of mean daily sea level pressure data in the NCEP-NCAR reanalysis and the Centre National de Recherches Météorologiques coupled global climate Model (CNRM-CM3) SRES A2 integration. Mid-latitude lows and highs traveling in the North Pacific were tracked and daily frequencies were gridded. Transient activity in the CNRM-CM3 historical simulation (1950–1999) was validated against reanalysis. The GCM correctly reproduces winter trajectories as well as mean geographical distributions of cyclones and anticyclones over the North Pacific in spite of a general under-estimation of cyclones' frequency. On inter-annual time scales, frequencies of cyclones and anticyclones vary in accordance with the Aleutian Low (AL) strength. When the AL is stronger (weaker), cyclones are more (less) numerous over the central and eastern North Pacific, while anticyclones are significantly less (more) numerous over this region. The action of transient cyclones and anticyclones over the central and eastern North Pacific determines seasonal climate over the West Coast of North America, and specifically, winter weather over California. Relationships between winter cyclone/anticyclone behavior and daily

precipitation/cold temperature extremes over Western North America (the West) were examined and yielded two simple indices summarizing North Pacific transient activity relevant to regional climates. These indices are strongly related to the observed inter-annual variability of daily precipitation and cold temperature extremes over the West as well as to large scale seasonally averaged near surface climate conditions (e.g., air temperature at 2 m and wind at 10 m). In fact, they represent the synoptic links that accomplish the teleconnections. Comparison of patterns derived from NCEP-NCAR and CNRM-CM3 revealed that the model reproduces links between cyclone/anticyclone frequencies over the Northeastern Pacific and extra-tropical climate conditions but is deficient in relation to tropical climate variability. The connections between these synoptic indices and Western weather are well reproduced by the model. Under advanced global warming conditions, that is, the last half of the century, the model predicts a significant reduction of cyclonic transients throughout the mid-latitude North Pacific with the exception of the far northern and northeastern domains. Anticyclonic transients respond somewhat more regionally but consistently to strong greenhouse forcing, with notably fewer anticyclones over the Okhotsk/Kamchatka sector and generally more anticyclones in the Northeastern Pacific. These modifications of synoptic weather result in regional feedbacks, that is, regional synoptic alterations of the anthropogenic warming signal around the North Pacific. In the eastern Pacific, for example, synoptic feedbacks, having to do especially with the northward shift of the eastern Pacific storm-track (responding, in turn, to a weaker equator-to-pole temperature gradient), are favorable to more anticyclonic conditions off the American mid-latitude west coast and more cyclonic conditions at higher latitudes. These circulation feedbacks further reduce the equator-to-pole

A. Favre (✉)
Center de Recherches de Climatologie (CRC),
Faculté des Sciences Gabriel, Université de Bourgogne,
21000 Dijon, France
e-mail: favre_alice@yahoo.fr

A. Gershunov
Climate Research Division, 0224,
Scripps Institution of Oceanography, UC San Diego,
La Jolla, CA 92093-0224, USA
e-mail: sasha@ucsd.edu

temperature gradient by favoring high-latitude mean winter warming especially over a broad wedge of the Arctic north of the Bering Sea and moderating the warming along the mid-latitude west coast of north America while also reducing precipitation frequencies from California to Northern Mexico.

1 Introduction

At global scale, during the last half-century, observed mid-latitude transient winter cyclones became less frequent, but more intense. The occurrence of deep cyclones increased significantly in both the Southern (e.g., Simmonds and Keay 2000a, b Pezza and Ambrizzi 2003) and the Northern (e.g., Serreze et al. 1997; Gulev et al. 2001) mid-latitudes since mid-twentieth century. While the number of mid-latitude (30°–60°N) lows diminished during this period, high latitude (north of 60°N) lows became more numerous in accordance with the general warming of the Northern Hemisphere (McCabe et al. 2001).

In the North Pacific, Graham and Diaz (2001) observed that strong extra-tropical cyclones gradually increased in number during the last five decades. This trend was accompanied by an eastward shift and an intensification of the Aleutian Low (AL) from the mid-1970s (e.g., Trenberth 1990; Trenberth and Hurrell 1994; Overland et al. 1999) coinciding with strengthened cyclonic activity and weakened anticyclonic activity in the Northeastern Pacific (Favre and Gershunov 2006, hereafter FG2006). The observed general strengthening of eastern North Pacific cyclonic activity went counter to global observations and most climate change projections for the mid-latitudes. Regionally, these observations coincide and are consistent with a general nighttime warming over the West (e.g., Karl et al. 1984, 1986, 1993; Easterling 2002; Groisman et al. 2004) and more frequent downpours over the southwestern United States after the mid-1970s (Gershunov and Cayan 2003). Were these observed regional synoptic changes purely natural? How are regional synoptic transients expected to evolve under global climate change? What does that bode for Western weather and climate? These questions motivate this work and are addressed below.

Most models project a general reduction of mid-latitude cyclones in response to global warming scenarios (e.g., Koenig et al. 1993; Lambert 1995; Lambert and Fyfe 2006; IPCC 2007). The principal reason evoked is the change in baroclinicity in the lower troposphere (e.g., Lambert 1995; Lunkeit et al. 1998; Yin 2005). These modifications could be induced by a reduced equator-to-pole temperature gradient due to stronger warming predicted for high-relative to low-latitudes and related factors

such as reduction of sea-ice extent (e.g., Holland and Bitz 2003; Sewall and Sloan 2004; Sewall 2005). This could lead to reduced baroclinic instability, which would be unfavorable to cyclogenesis. Nevertheless, in a warming atmosphere, the models predict increasing humidity. The enhanced potential for latent heat release could reinforce the deepest cyclones, making deep lows more numerous while moderate events decline (Lambert 1995; Lambert and Fyfe 2006).

As for mid-latitude transient anticyclones, few studies address their features, and evolution in a changing climate. Considering Northern Hemisphere winter climate warming in the NCAR Community Climate Model version 1, Zhang and Wang (1997) found that a decrease of cyclone frequencies was accompanied by a similar decrease in the frequency of transient anticyclones.

Furthermore, studies of possible regional climate change, suggest a more moderate winter warming of the West compared to the inner North American continent (IPCC, 2007) as well as less precipitation over the southwestern US and northern Mexico but more in the Northwest and western Canada (e.g., Sewall and Sloan 2004; Sewall 2005; IPCC 2007).

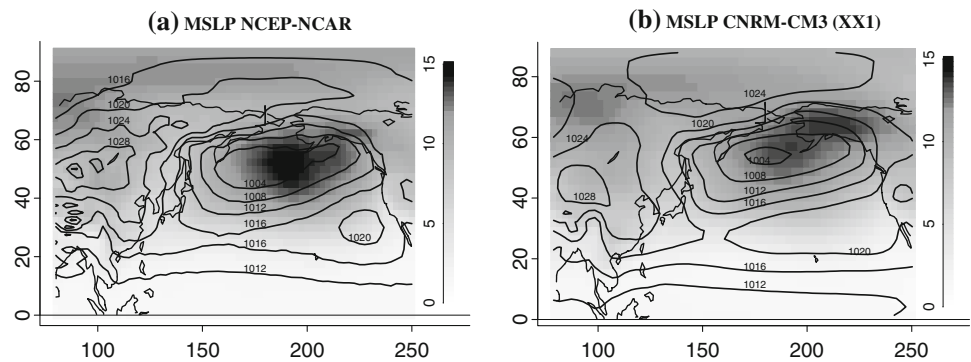
Regional weather and climate variations in mid-latitudes (e.g., occurrence of precipitation, cold waves, etc.), specifically during winter, depend directly on transient synoptic features (e.g., FG2006). Thus, the study of possible evolution of regional transient activity in models provides the opportunity to envisage the synoptic nature and dynamics of regional climatic evolution. In this work, we will analyze how the winter climatology of North Pacific mid-latitude surface cyclones and anticyclones could evolve in the context of global warming and what consequences are foreseen for winter weather over the West.

The paper is arranged as follows: Sect. 2 presents the data and methodology; Sect. 3 describes the climatology of North Pacific cyclones and anticyclones; Sect. 4 considers the modeled consequences of global warming projected on the North Pacific transient activity; and Sect. 5 discusses the possible impacts of these changes on regional weather over the West. Summary and conclusions are presented in the last section.

2 Data and methodology

To quantify surface cyclonic/anticyclonic activity and to study how global warming could influence transient behavior over the North Pacific, we have first constructed trajectories of transient highs and lows, from observations and GCM simulations of mean daily sea level pressure. Using the daily-resolved trajectories, we gridded and

Fig. 1 Winter (JFM) mean sea level pressure (contours) and inter-daily variation of sea level pressure (*shading*, expressed in hPa), from reanalysis (a), and from the model historical simulation (b). Contour interval is 4 hPa



studied seasonal frequency fields of cyclonic and anticyclonic transients.

2.1 Observed and modeled data

North Pacific mid-latitudes transient activity is analyzed from daily mean sea level pressure (MSLP, JFM 1950–2001) obtained from NCEP-NCAR reanalysis (Kalnay et al. 1996; Kistler et al. 2001) and from the Center National de Recherches Météorologique Coupled general circulation Model version 3 (CNRM-CM3: Salas-Mélia et al. 2005). The CNRM-CM3 is a coupling of the Atmospheric Global Model ARPEGE-Climat version 3 (Déqué et al. 1999; Gibelin and Déqué 2003), the OPA8.1 ocean model (Madec et al. 1998), GELATO2 sea ice model (Salas-Mélia 2002), ISBA land surface scheme (Noilhan and Planton 1989; Mahfouf et al. 1995; Douville et al. 1995a, b) and TRIP river routing scheme (Oki and Sud 1998; Chapelon et al. 2002). This global spectral model has a spatial resolution of T63 (about $1.9^\circ \times 1.9^\circ$) with 45 vertical levels. Two simulations of the CNRM-CM3 are used: a historical simulation (XX1) covering the period 1860–1999 with observed radiative forcing (annual mean), and the climate change simulation, for the period 2000–2099, which conforms to the SRES A2 business-as-usual-type scenario (IPCC 2007). From these two simulations, we have restrained our analysis to the 1950–1999 and 2050–2099 periods, permitting, on the one hand, the model comparison with reanalysis and reinforcing, on the other hand, the analysis results with two contrasted periods of advanced versus observed global warming.

2.2 Comparison of reanalyzed and modeled winter MSLP fields

Preliminary analysis of North Pacific winter MSLP reveals that the mean configuration of North Pacific atmospheric centers of action (Aleutian Low and sub-tropical High) is similar in reanalysis and in the model historical simulation.

Nevertheless, a light overestimation of mean pressures in the model, as compared with reanalysis (Fig. 1a, b), affects the whole region, except for the Asian continent, where pressures are underestimated. Consequently, the modeled AL is somewhat retracted, specifically in the south, to the benefit of subtropical high-pressure influence between 20°N and 40°N . The day-to-day variability of pressure is relatively well modeled but is under-estimated over the Aleutians and the Gulf of Alaska, and overestimated over Alaska.

The analysis of transient trajectories will clarify how these differences in the mean field of MSLP appear at synoptic timescale.

2.3 Constructing trajectories of transient highs and lows

Trajectories of transient cyclones and anticyclones were established from NCEP-NCAR reanalysis, CNRM-CM3 historical and SRES A2 simulations of MSLP, using an automated scheme presented below.

From daily MSLP, we have constructed surface transient trajectories using the tracking algorithm presented in FG2006. The automated scheme first recognizes and determines the spatial position of each local minima/maxima of MSLP, inferior/superior to 1,005 hPa/1,015 hPa, defining surface cyclone/anticyclone centers, respectively. The local partial derivatives, zonal and meridional, permit to identify these minima and maxima of pressure in the four cardinal directions. Next we retain the coordinates of each minima below 1,005 hPa (cyclones) and maxima above 1,015 hPa (anticyclones). These centers of low and high pressure are tracked, day after day according to their temporal pressure variations and spatial displacement criteria described in FG2006.

The geographical domain in which trajectories are constructed covers the $0^\circ\text{--}90^\circ\text{N}/80^\circ\text{E--}110^\circ\text{W}$ region. The Rocky Mountains represent the eastern limit: transients circulating to the east of this topographic barrier do not

directly affect the North Pacific Basin. To the West, East Asia is included in our analysis, because any transients that circulate in the North Pacific Basin can originate and/or transit over this region, before entering the ocean basin: this is especially true for anticyclones during winter season.

In this study we analyze transients having a lifetime of 2 days at least, transiting in the 30°N–60°N zone, and circulating over the North Pacific Basin during one day at least. In this way, we consider only mid-latitude features and exclude transients that circulate exclusively to the north of 60°N or to the south of 30°N. Nevertheless, trajectories which circulate over the North Pacific during one day at least, are recorded in their totality; consequently they can generate, decay or transit temporarily outside of this core region.

2.4 Mapping the frequency of transient features

Mapping the frequency of transient features is a delicate procedure (e.g., Zolina and Gulev 2002). The choice of space–time resolution for data used to construct transient trajectories can produce biases in frequency mapping. The origin of the problem is two-fold.

First, a coarse space–time resolution does not permit to precisely record the real life-time of trajectories (from genesis to decay). In this study, the algorithm detects closed systems in MSLP fields, thus, at the stage of genesis, a higher space–time resolution should permit to detect the systems earlier, and follow them further into the stage of decay. Consequently, the space–time resolution influences the duration of trajectories, as well as the system frequencies per cell. Our analysis is limited by coarse space–time resolution that will be improved upon in subsequent studies. Nevertheless, results presented below reflect regional climates modifications that could be attributed to a change of mid-latitude transient activity, due to global warming.

The second problem is related to the relative punctuality of recording position of transients on a grid. A rapid displacement of an atmospheric center will not be recorded in the same way as a slow (or a non-) displacement, with an under- and over estimation of occurrence per cell, respectively. According to the objective of the study, it is more or less necessary to adjust to this problem by treating transit and duration separately. In this work as in Lambert (1995), we assume the over-representation in space of slow or blocked systems, because, our analysis addresses general cyclonic and anticyclonic activity, so the notion of duration is as important as that of transit. Our principal concern is to obtain homogenous spatial structure with a reasonable number of observations per cell. Consequently we have to adapt the spatial frequency grid resolution to the source data space–time resolution used for the tracking step. Because of our choice of daily MSLP data (daily time

step), a coarse spatial resolution is appropriate for the frequency analysis. Accordingly, we chose a 10°*10° grid to summarize cyclone/anticyclone frequencies for each winter in reanalysis as well as in CNRM-CM3 simulations. The relatively coarse grid-resolution avoids interpolation, while obtaining homogeneous mean spatial structures.

3 Winter climatology of North Pacific transients

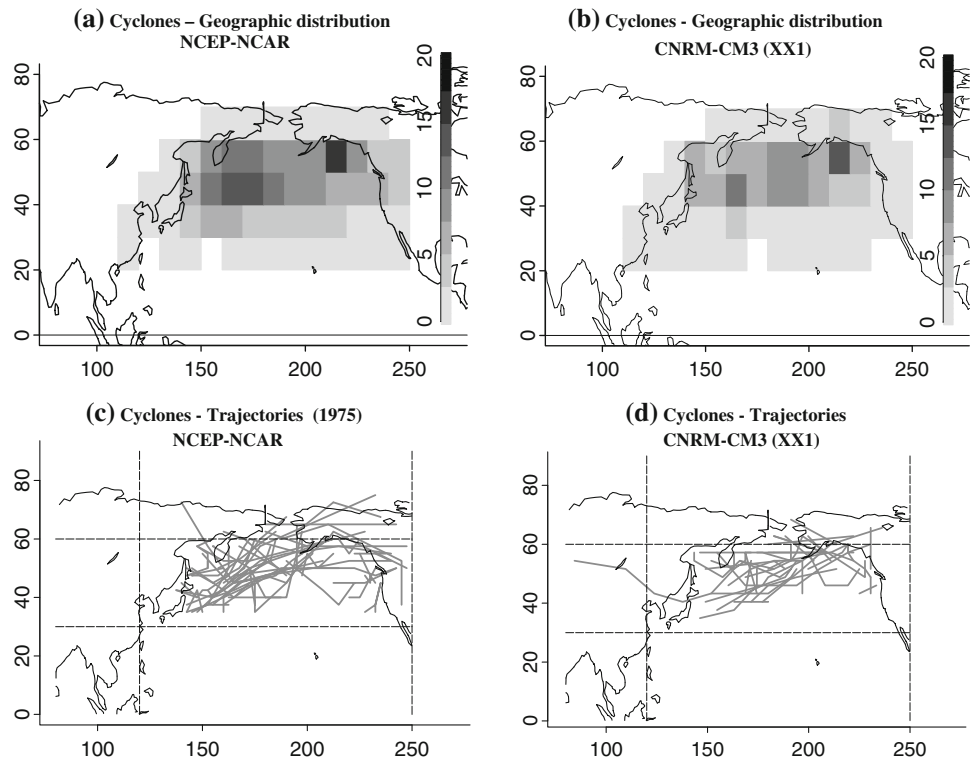
The general comparison of transient climatology derived from reanalysis and the model will permit to verify that, in spite of the seasonal mean over-estimation of MSLP, the model is apt to correctly reproduce trajectories as well as the geographical patterns of mid-latitude transient cyclonic (Sect. 3.1) and anticyclonic (Sect. 3.2) activity.

3.1 Cyclonic activity

On seasonal winter average, the principal zone of cyclonic center passages extends between 30°N and 60°N and they are most frequent between 40°N and 60°N (Fig. 2a, b). In both observations and model, there are two principal centers of cyclonic activity: to the southeast of Kamchatka and in the Gulf of Alaska. This is consistent with previous studies (e.g., Pettersen 1956; Anderson and Gyakum 1989; Geng and Sugi 2003).

Figure 2c and d presents samples of typical winter cyclone trajectories derived from reanalysis and model data (for “normal” winters). Normally, trajectories tend to occupy a large band stretching east of Japan to the Gulf of Alaska and passing to the South of Kamchatka and over the Aleutian Islands. The latitudinal domain of cyclonic circulation is distinctly larger in the western part of North Pacific, with cyclones circulating further south than in eastern part of the basin, where trajectories tend to be more confined in the Gulf of Alaska (e.g., Pettersen 1956; Klein 1957; Hanson and Long 1985; Gyakum et al. 1989; Zhang and Wang 1997; Gulev et al. 2001; Lambert et al. 2002). The western Pacific sector is favorable to cyclogenesis (not shown) and previous studies point out the Kuroshio influence as a favorable factor for intensification to the east of Japan (e.g., Sanders and Gyakum 1980; Roebber 1984, 1989; Rogers and Bosart 1986; Gyakum et al. 1989; Gulev et al. 2001). These cyclones have long lifetimes and move rapidly north-east-ward (Zolina and Gulev 2002), towards the Aleutians and the Gulf of Alaska and merge into the statistical AL (Wallace et al. 1988; Gulev et al. 2001). The Gulf of Alaska is also a favorable area for cyclogenesis and intensification (e.g., Reed and Albright 1986). Nevertheless, the particularity of this region is that it is also favorable to the decay (not shown) of cyclones (Gulev et al. 2001; Martin et al. 2001; McLay and Martin 2002).

Fig. 2 Mean cyclones' frequency per $10^{\circ} \times 10^{\circ}$ cell (a, b). Cyclone trajectories during a normal winter (c, d) from the NCEP-NCAR reanalysis (left panels) and the model historical simulation (right panels). Normal winter = total number of trajectories near the normal and spatial repartition of frequencies near the normal

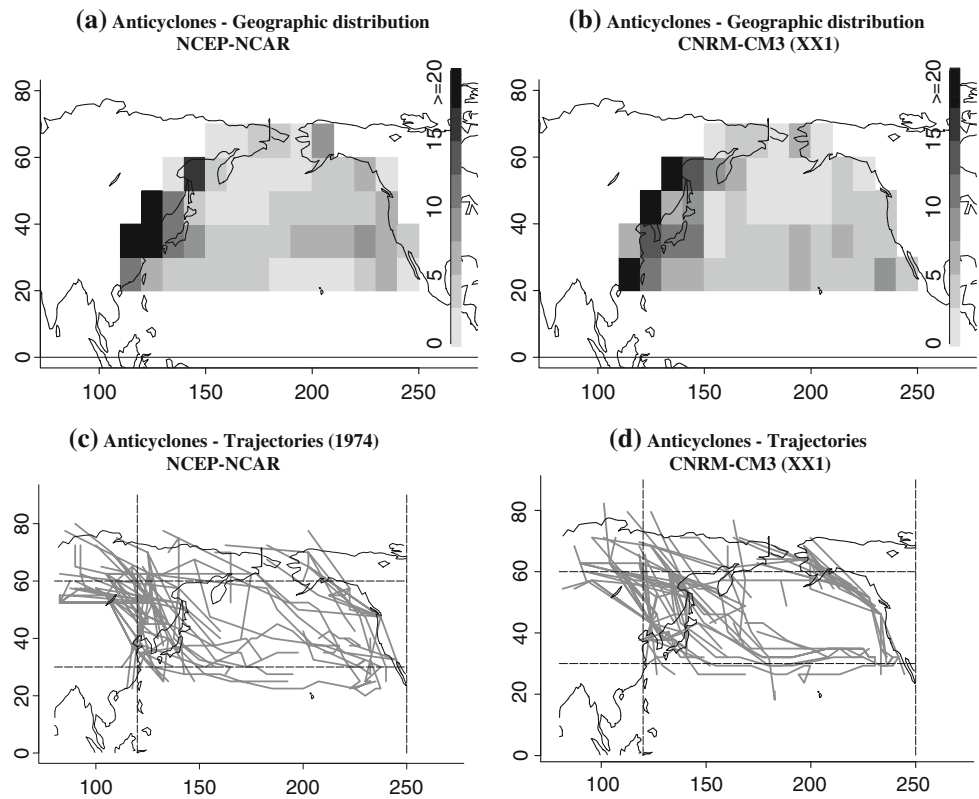


Over the southwest coast of the United States, the occurrence of lows is relatively infrequent because of the subtropical high's influence limiting the generation and/or propagation of cyclones in latitudes inferior to 45°N – 40°N . Regions to the south of 40°N are most often influenced by the tail ends of Gulf storms landing around British Columbia. Occasionally, however, cyclones can also generate between Hawaii and the continent. These rare “Pineapple Express” storms typically arrive well-centered to California (e.g., Dettinger et al. 2004; Ralph et al. 2004).

In the modeled historical simulation, the trajectories and the mean spatial structures of cyclones' frequency are correctly reproduced, but frequency is generally underestimated. Cyclonic trajectories are less numerous over the basin (40 modeled compared to 66 observed per average winter: -33%) in the GCM compared to reanalysis. This model underestimation is strongly pronounced over the Northeastern Pacific and in latitudes inferior to 40°N . Nevertheless cyclones in the model have a longer mean life-time with 4.34 days against 3.79 days in reanalysis ($+13\%$). In spite of a greater duration, the mean cyclone occurrences (impacts per cell) are under-estimated in the model. In the mid-latitude North Pacific (30°N – 60°N), cyclone occurrences per cell are under-estimated by approximately 30% in the model in comparison with reanalysis. We have thought that the MSLP difference between reanalysis and the model and the choice of the fixed-threshold (1,005 hPa) for identification of cyclones

are perhaps the causes of this model under-estimation. After a simple verification, the number of local pressure minima detected in the model, without imposed threshold, is around 30% below that in the reanalysis (keeping in mind the spatial resolution difference). Lambert and Fyfe (2006) have equally found that cyclonic events are underestimated by approximately the same percentage in the CNRM-CM3 in comparison with ERA40 reanalysis, for the Northern Hemisphere. Moreover, in the model, central pressure of cyclones is generally higher than in reanalysis by around 4 to 5 hPa (not shown). For example the minimum central pressure reached by all mid-latitude cyclones over the North Pacific is 985 hPa (on average) in reanalysis and 990 hPa in the model. Lambert et al. (2002) have suggested that the mean field of pressure results from the respective contribution of transient lows and highs. Thus, the simulation errors of seasonal mean pressures are generally associated with a surplus or a deficit of cyclone occurrences as well as with their relative depression. Consequently the over-estimation of MSLP in the model (Fig. 1) could be caused, at least in part, by the generally weaker transient cyclonic activity in the model (Fig. 2) and specifically in latitudes inferior to 40°N (-80%) and over the Northeastern Pacific. The Rocky Mountains play an important role on the North Pacific cyclonic activity, blocking transients along the coast. Because of the relatively coarse resolution used by models, transient cyclones are not sufficiently confined specifically in the Gulf of

Fig. 3 Mean anticyclones' frequency per $10^{\circ} \times 10^{\circ}$ cell (a, b). Anticyclone trajectories during a normal winter (c, d) from reanalysis (left panels) and from the model historical simulation (right panels)



Alaska. This causes an excessively northward location of the AL (IPCC 2007) to the benefit of subtropical high pressures, which are generally too strong in models (e.g., Lambert et al. 2002).

3.2 Anticyclonic activity

The number of high trajectories reaching the North Pacific mid-latitudes is similar in the model and observations (117 versus 115 per average winter). Their life-times are also well-simulated (3.61 versus 3.63 days) as well as the mean spatial structures of anticyclonic activity (Fig. 3). The anticyclonic trajectories are highly concentrated over the west part of our sector. During winter, the Siberian High favors frequent cold air discharges over the Okhotsk, Japan, and China Seas regions (e.g., Jhun and Lee 2004; Panagiotopoulos et al. 2005). These cold air outbreaks form ridges of pressure, which can develop into closed anticyclones over the ocean and propagate south-eastward to the subtropical latitudes. These synoptic phenomena are associated with the winter monsoon (cold and dry north winds) over southeastern Asia and the western North Pacific. Around 75% of mid-latitude anticyclones, which reach the North Pacific Basin, are generated over the Asian continent but decay rapidly over the western North Pacific. Under the influence of cyclonic displacement, some of them can propagate zonally and

reach the eastern North Pacific. This happens to around 10% of Asian anticyclones. Another category of transient anticyclones wander over the far-eastern Siberia, Bering Sea or Alaska, and drop directly into the Northeastern Pacific, propagating along the coast of North America. These transients are associated with cold air outbreaks over the Pacific Northwest (FG2006). Mid-latitude anticyclones tend to merge with the sub-tropical high (Wallace et al. 1988). According to this general description, North Pacific anticyclones are most frequent along the Asian continent and to a lesser extent, along the west coast of North America. Transient anticyclones are distinctly rare in the AL area. These observations are in accordance with Pettersen (1956) and later studies.

On average anticyclones are more (less) numerous over East Asia (Northeast Pacific) in the model in comparison with reanalysis.

Summarizing this section, we have verified the model's capacity to reproduce the mean climatology of transients in the North Pacific Basin. It is recognized that in spite of an under-estimation of cyclones' frequency and intensity, the model historical simulation correctly reproduces the mean features of mid-latitude transients, trajectories, as well as the spatial distribution of mean frequency. A notable exception seems to be a severe model under-estimation of cyclonic intrusions into the Pacific Northwest and at latitudes inferior to 40°N .

4 North Pacific transient activity: observations and modeled consequences of projected global warming

On inter-annual time scales, the seasonal mean AL reveals tropospheric circulation variations over the North Pacific Basin. A deep AL in winter reflects and promotes a cyclonic circulation anomaly over the North Pacific as well as warmer temperatures along the American West coast and colder temperatures over the central North Pacific. Opposite anomalous conditions prevail over the region when AL is weak. Variations of the AL influence western North American climate especially during winter (e.g., Wallace and Gutzler 1981; Barnston and Livezey 1987). This mean statistical Low varies with mid-latitude high frequency weather features, explicitly with respect to synoptic cyclonic and anticyclonic transient activity (e.g., FG2006, Zhu et al. 2007).

Zhu et al. (2007) have estimated the effect of extratropical cyclones on the inter-annual variability of the winter mean AL. They have distinguished two types of preferred cyclonic trajectories that account for the strong and weak phases of the AL intensity. A strong AL corresponds to a zonal displacement of cyclones with tracks closely following each other and high concentration over and to the east of the Aleutian Islands. Conversely, during winters marked with an anomalously weak AL, cyclones tend to be disorganized over the entire North Pacific Basin favoring more meridian trajectories with a stronger pole-ward component.

In order to estimate the capacity of the model to reproduce the general features of transient activity's low-frequency variability, we first describe how cyclones and anticyclones co-vary with the AL in observations and model (Sect. 4.1).

According to previous studies (e.g., Koenig et al. 1993; Lambert 1995; Lambert and Fyfe 2006; IPCC 2007), global warming should restrain transient cyclones in mid-latitudes

but encourage them at higher latitudes. Nevertheless uncertainties endure about future AL evolution (IPCC 2007). Many models project a pole-ward displacement and an intensification of the AL (IPCC 2007). In Sect. 4.2, possible changes in transient activity and AL will be analyzed in the SRES A2 simulation.

4.1 Transient activity and Aleutian Low variability: comparison between observations and historical simulation

We have, in the previous section, verified that the spatial distribution of cyclonic and anticyclonic trajectories and associated mean frequencies are correctly reproduced in the model historical simulation. Now, we will describe transient cyclonic and anticyclonic behavior according to the strong and weak phases of the AL in reanalysis and in the model. First, we have constructed the AL strength index, that is, winter SLP averaged over the 30°N–60°N/150°E–140°W region, and then we classified strong and weak AL winters in reanalysis and model historical simulation (Fig. 4).

In observations, the AL index presents a significant shift between 1976 and 1977. From 1977, the AL is deeper in average (mean difference between 1977 and 2001 and 1950–1976 = -3 hPa, t -test sig. $>99\%$) and more variable ($+1.2$ hPa for the standard deviation, F -test sig. $>95\%$). In the historical simulation no significant change of the AL strength is detected.

During strong AL winters, cyclones are more frequent over the central and eastern North Pacific and off California but less numerous over the Kamchatka sector and off British Columbia (Fig. 5a, b). This anomalous configuration of cyclonic activity is associated with fewer anticyclones over the central and eastern part of the North Pacific Basin but more over the west and south of 30°N (Fig. 6a, b).

Fig. 4 Time series of mean SLP over the 30°N–60°N/150°E–140°W zone derived from reanalysis (1950–2001) (a), and from the model historical (XX1 from 1 to 50) and SRES A2 (from 51 to 100) simulations (b). Solid and dashed horizontal lines represent means and standard deviation intervals, respectively

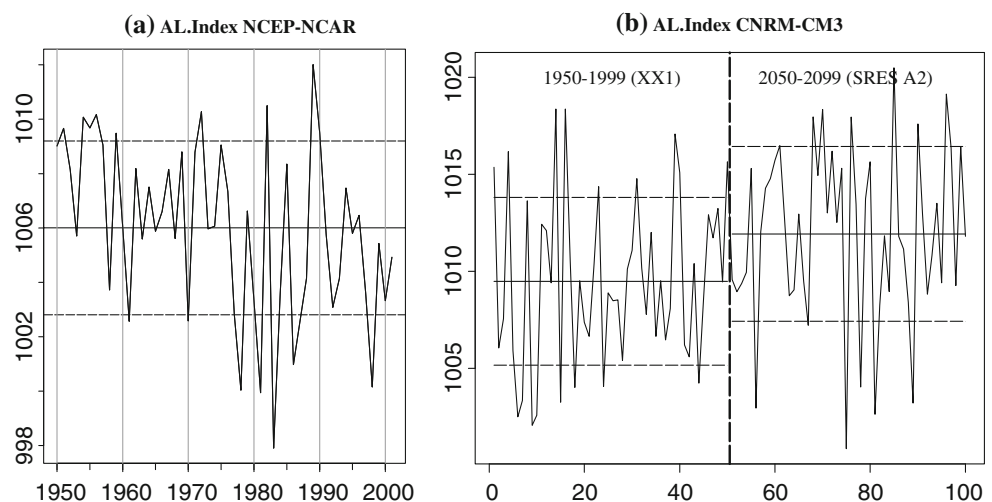


Fig. 5 Cyclones frequency (shading) during strong (above) and weak (below) Aleutian Low phases in reanalysis (left panels) and in the model historical simulation (right panels). Composites are constructed with the standard deviation method. Signs ±: difference with mean field, sig. >90% and bold signs = sig. >95% (bootstrap test 1,000 samples chosen at random)

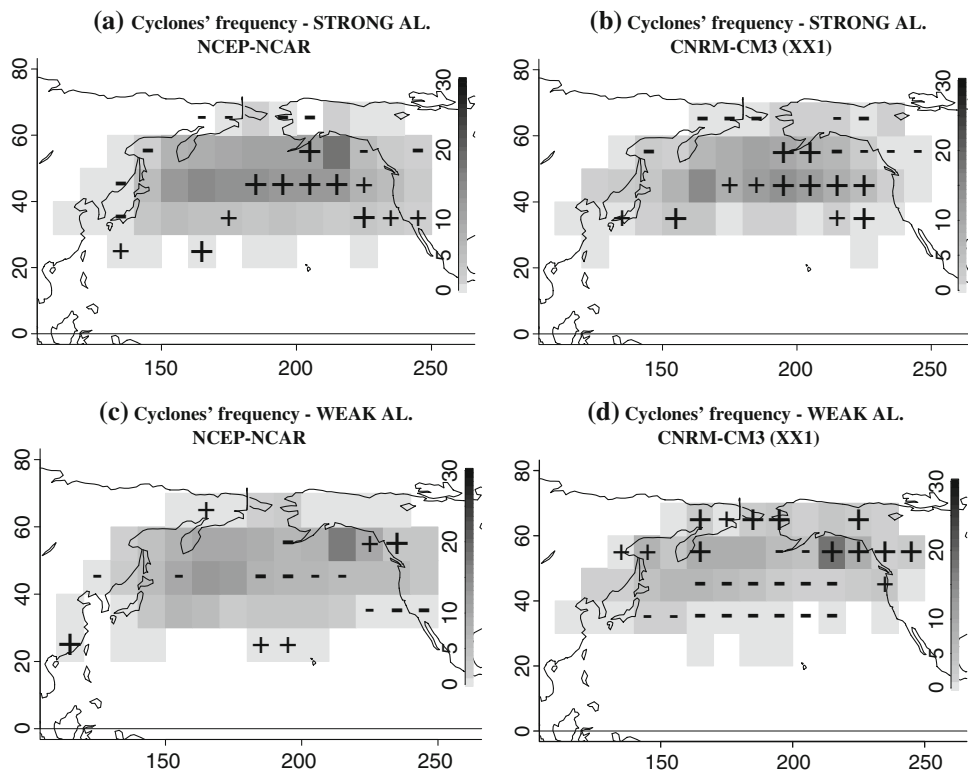
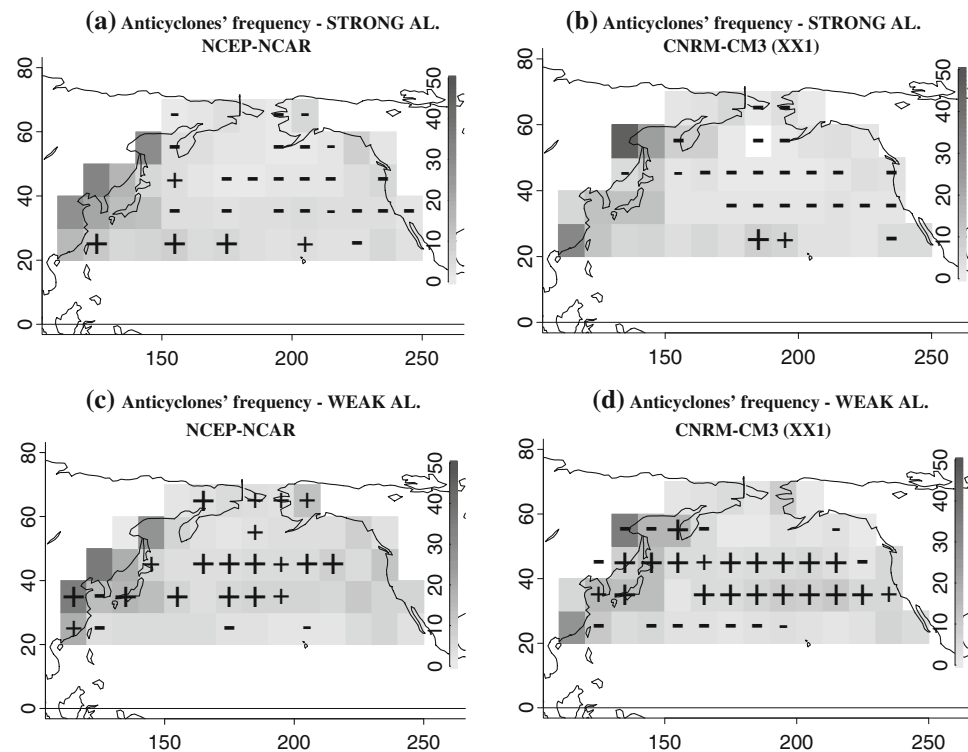


Fig. 6 Same as Fig. 5, but for anticyclones



When AL is weak, cyclones are less numerous over the eastern Aleutians and between Hawaii and California, but their frequency is reinforced in the Gulf of Alaska/ British Columbia sector (Fig. 5c, d). Anticyclones are

then generally more numerous in the mid-latitudes (Fig. 6c, d).

The model correctly reproduces these general anomalies but we note that during the weak AL phase, the model's

cyclonic activity is reduced over much of the 30°N–50°N band, while in reanalysis, the reduction concerns preferentially the eastern AL area and the sector between Hawaii and California. The same remark can be made for anticyclonic activity during the positive AL phase when transient highs are less numerous in the 30°N–50°N band in the model, while in reanalysis, this reduction is most significant specifically over the central and eastern mid-latitude North Pacific.

Thus, in the mid-latitude North Pacific, frequencies of cyclones and anticyclones vary generally inversely according to AL phase. In fact, high and low transient frequencies are negatively correlated ($r = -0.71$, sig. >99% in the reanalysis and $r = -0.60$, sig. >99% in the GCM). Consequently, an intensified transit of cyclones is unfavorable to anticyclonic formation and/or propagation over the mid-latitudes and specifically over the East. This anti-correlation is greatest ($r = -0.84$, sig. >99% in the reanalysis and $r = -0.70$, sig. >99% in the GCM), specifically, in the eastern part of the AL area (180°–130°W/40°–60°N). This anti-phase could be due to the fact that when cyclones are more numerous they are closer to each other (e.g., Zhu et al. 2007) and this could inhibit the generation and/or propagation of anticyclones, which tend to follow low pressure systems, that is, hindering pressure ridges from organizing themselves into closed mid-latitude systems.

In summary, the model appears capable to correctly reproduce the general inter-annual variability of cyclonic and anticyclonic activity in accordance with AL phases.

4.2 Projected anthropogenic impacts on the AL and transient activity

In the global warming scenario, the model projects higher MSLP in the entire North Pacific and especially in the East (Fig. 7). Conversely, lower MSLP is projected for the higher latitudes, across Siberia and in the Arctic Basin, particularly over Laptev, Eastern Siberia, and Chukchi Seas. Temperatures are generally higher everywhere but with regional nuances related to mean projected changes in circulation. The warming is projected to be strongest over the Arctic Basin and Siberia and this feature is common in many model projections, as well as in observations of contemporary global warming (e.g., IPCC 2007). In the North Pacific, the rising pressure induces anticyclonic circulation anomalies centered over the east (roughly 40°N–150°W) resulting in weaker mid-latitude westerlies. Along the west coast of North America, northerly wind anomalies moderate the projected warming from the Gulf of Alaska to California and, inversely, along the Asian coast, southerly wind anomalies encourage the warming from the Okhotsk Sea to the Bering Strait.

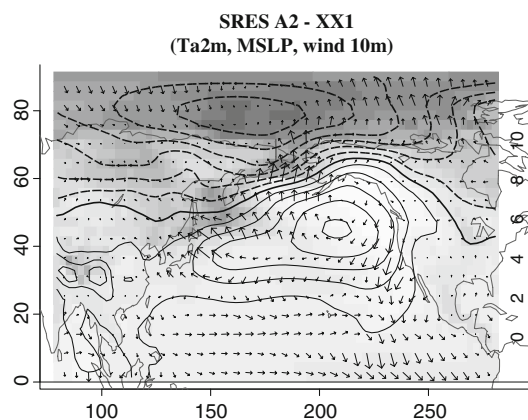


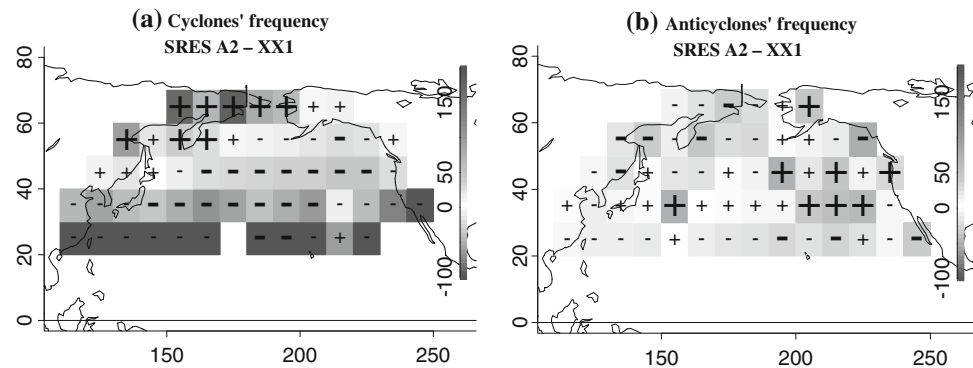
Fig. 7 Difference between SRES A2 and historical simulation for Ta2 m (shading: °C), wind10 m (vectors) and MSLP (contour interval is 1 hPa, continue = positive, dashed = negative, bold = 0 hPa)

In the GCM SRES A2 scenario, the geographical mean frequency structure of cyclones is unchanged (not shown). Nevertheless, the number of cyclone trajectories, which reach the mid-latitudes of the North Pacific, is slightly lower with a reduction of about 7.5%. Their total lifetime is unchanged in general but significantly reduced south of 60°N by around 13%. Thus, on average, cyclones become significantly less numerous in the mid-latitude North Pacific from the China Sea to the Gulf of Alaska and especially at lower latitudes (Fig. 8a). Conversely, transient lows tend to be significantly more numerous along the Asian coast, from the Northern Sea of Japan to the Bering Strait and especially over the Siberian far east.

The projected number of anticyclonic trajectories that reach the mid-latitude North Pacific is reduced by about 8%, but their average lifetime is unchanged (not shown). Regionally, anticyclone frequency (Fig. 8b) is significantly reduced over the Okhotsk Sea, Kamchatka, and the eastern Bering Sea. Anticyclones are generally projected to be less numerous at lower latitudes, especially around Hawaii. Inversely, anticyclones' frequency is reinforced to the East of Japan, in the Northeastern Pacific between 30° and 50°N and over Alaska.

These modifications of surface transient activity and particularly reduced cyclonic activity in the mid-latitudes reflect stronger mean sea level pressure over the North Pacific and a weaker AL (Fig. 4b, for the AL Index: mean difference between SRES A2 and XX1 = +2.4 hPa, t -test sig. >99%, no significant difference in the variance). The southerly and the northerly components of the surface wind are intensified along the Asian coast and the west coast of Northern America, respectively. Thus, over the North Pacific Rim, the projected warming is accentuated in the West, and de-emphasized in the East, including the mid-latitude North American West Coast. In spite of the mean strength reduction of the AL, the inter-annual variability is

Fig. 8 Difference between cyclones (a), and anticyclones (b), frequency derived from the SRES-A2 and historical simulation, expressed in percentage (shading: percentage; larger signs \pm = sig. >95%, bootstrap test)



projected to remain strong, so that extreme cyclonic/anticyclonic winters should still be possible, but less/more likely, respectively (Fig. 4b).

These general changes, if they take place as projected, could have significant impacts on the western North American climate, expressed in temperature and precipitation regimes.

To better understand the effects of climate change on regional weather, we now focus our study on the eastern North Pacific and analyze how the frequencies of cyclones and anticyclones could vary in a global warming context and what impacts on regional daily precipitation and temperature are likely over western North America. But first, connections between synoptic transient activity and daily precipitation and temperature over western North America, associated with large scale seasonal mean low-frequency climate variability in the model historical simulation, will be verified by comparison with reanalysis.

5 Possible consequences of global warming on western North American climate via changes in cyclonic/anticyclonic activity

In the mid-1970s, the North Pacific/North American winter climate conditions were suddenly modified in accordance with the AL and the North Pacific Decadal Oscillation (NPO or PDO) shift (e.g., Mantua et al. 1997). Synoptic cyclonic activity over the northeastern Pacific was notably intensified to the detriment of anticyclonic activity (FG2006). Western North American winters warmed because southerly advection became more frequent particularly along the coast from Mexico to Alaska. Thus, over the continent, extreme cold temperatures, especially during nights became less frequent but warm extremes more frequent (FG2006).

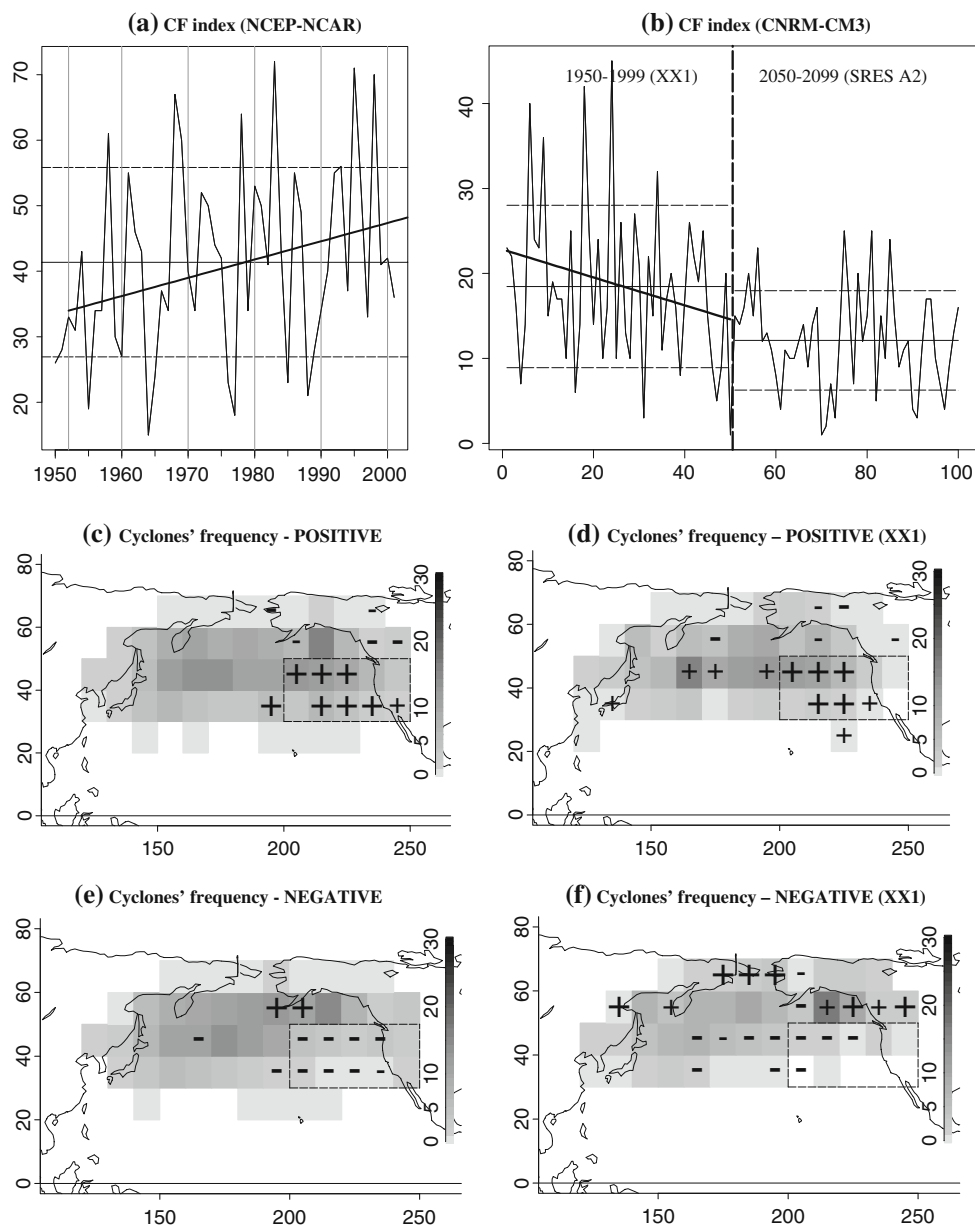
In Sect. 5.1, relationships between transient frequencies over the Northeastern Pacific and daily precipitation and temperature variability over western North America are summarized. Daily data from 276 stations distributed over

North America to the West of 100°W , covering the period 1950–2001 were obtained for the US (NCDC 2003), Canada (Vincent and Gullett 1999) and Mexico (Miranda 2003) from the National Climatic Data Center. Two indices synthesizing cyclonic and anticyclonic transient frequencies are derived and presented in Figs. 9a and 12a. These regional indices summarize transient activity intimately related with observed daily precipitation and extreme cold temperature frequencies (nightly temperatures (T_{min}) colder than the tenth percentile of all local T_{min} during winters 1950–2001) as recorded at stations over western North America. These observed relationships are presented in Figs. 11 and 14. Relationships between these two indices and global climatic fields, for example, MSLP, $T_{\text{a}} 2 \text{ m}$, and wind10 m, are also established in Figs. 10 and 13. These indices are then derived in model data (Figs. 9b, 12b) and next projected into the second half of the twenty first century and analyzed (Sect. 5.2).

5.1 North Pacific transient activity linking large-scale climate patterns to daily weather over the West

The CF index (Fig. 9a, b) summarizes cyclone frequencies off the US west coast (30°N – $50^{\circ}\text{N}/160^{\circ}\text{W}$ – 110°W , by simply counting cyclones in this area). Observed time series present high inter-annual variability of cyclone frequencies with maxima during winters 1958, 1968, 1969, 1978, 1983 (the maximum: 72), 1995, and 1998, contrasted with minima in winters 1950, 1955, 1964 (the minimum: 15), 1976, 1977, 1985, and 1988. Superimposed on these strong variations, a moderate, but significant, linear trend shows that regional daily cyclone frequency increased by about three cyclones per decade over this observational period. The model, as we have specified before, underestimates transient cyclone frequencies, specifically over the Northeastern Pacific and at lower latitudes. In this study area (30°N – $50^{\circ}\text{N}/160^{\circ}\text{W}$ – 110°W), the mean winter frequency of modeled transient cyclones in the historical simulation is 19 (standard deviation: 10), against 41 (standard deviation: 14) in observations, so the inter-annual

Fig. 9 The CF index is computed summarizing daily occurrences of transient cyclones in the area delimited on (c, d, e, f) from reanalysis (a) and (b) from the model historical simulation (XX1: from 1 to 50) and the SRES-A2 simulation (SRES A2: from 51 to 100). *Solid and dashed horizontal lines* represent means and standard deviation intervals, respectively, and *bolded line* the linear trend (reanalysis: +2.8 per decade; XX1: -2 per decade, sig. >95%). Positive composite (c, d) and negative composite (e, f) constructed from CF index (standard deviation method). *Shading*: cyclones frequency; *signs ±*: difference with mean field, sig. >90% and *bold signs* = sig. >95% (bootstrap test 1,000 samples chosen at random)



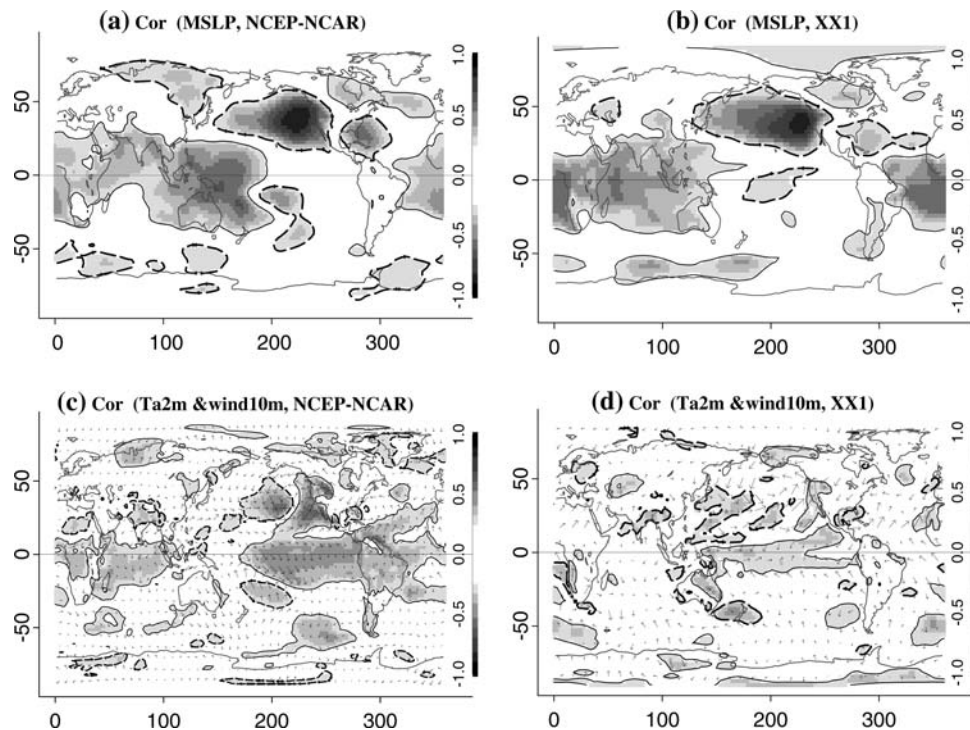
variability is higher relative to the mean in the model than in reanalysis. Moreover, the model historical simulation shows a decreasing linear trend in cyclonic frequency, that is, opposite to the observed trend. We note that the model historical run cannot be expected to reproduce observed PDO shifts. We hypothesize that the 1976–1977 PDO shift went counter to the regional trend that we can expect from global warming based on modeling results. The moderate modeled decrease in cyclonic frequency of about two regional cyclones per decade will be discussed below.

The cyclonic frequency composites reveal relatively symmetric patterns between the high and low CF index winters, in observations (Fig. 9c, e) and in the model (Fig. 9d, f). When transient lows are more numerous off

the US west coast, they circulate less often over higher latitudes: near Alaska and British Columbia. Inversely when lows are less frequent between 30°N and 50°N, they are more frequent around the Alaska Peninsula in observations, but the response is subtly different in the model with more cyclones in the Gulf of Alaska and over British Columbia.

Linear correlations between the CF index and global climatic fields (Fig. 10) show that regional synoptic transient cyclonic activity varies in accordance with mean winter atmospheric conditions over the Pacific Basin. The model is able to reproduce many details of global MSLP teleconnections with regional CF index as revealed in observations (Fig. 10a, b), excepted perhaps for the

Fig. 10 Linear correlations between CF index and MSLP (a, b), Ta2 m and wind10 m (c, d). Shading = significant correlation (>95%), continue lines = positive values, dashed lines = negative values. Left panels: NCEP-NCAR, right panels: CNRM XX1

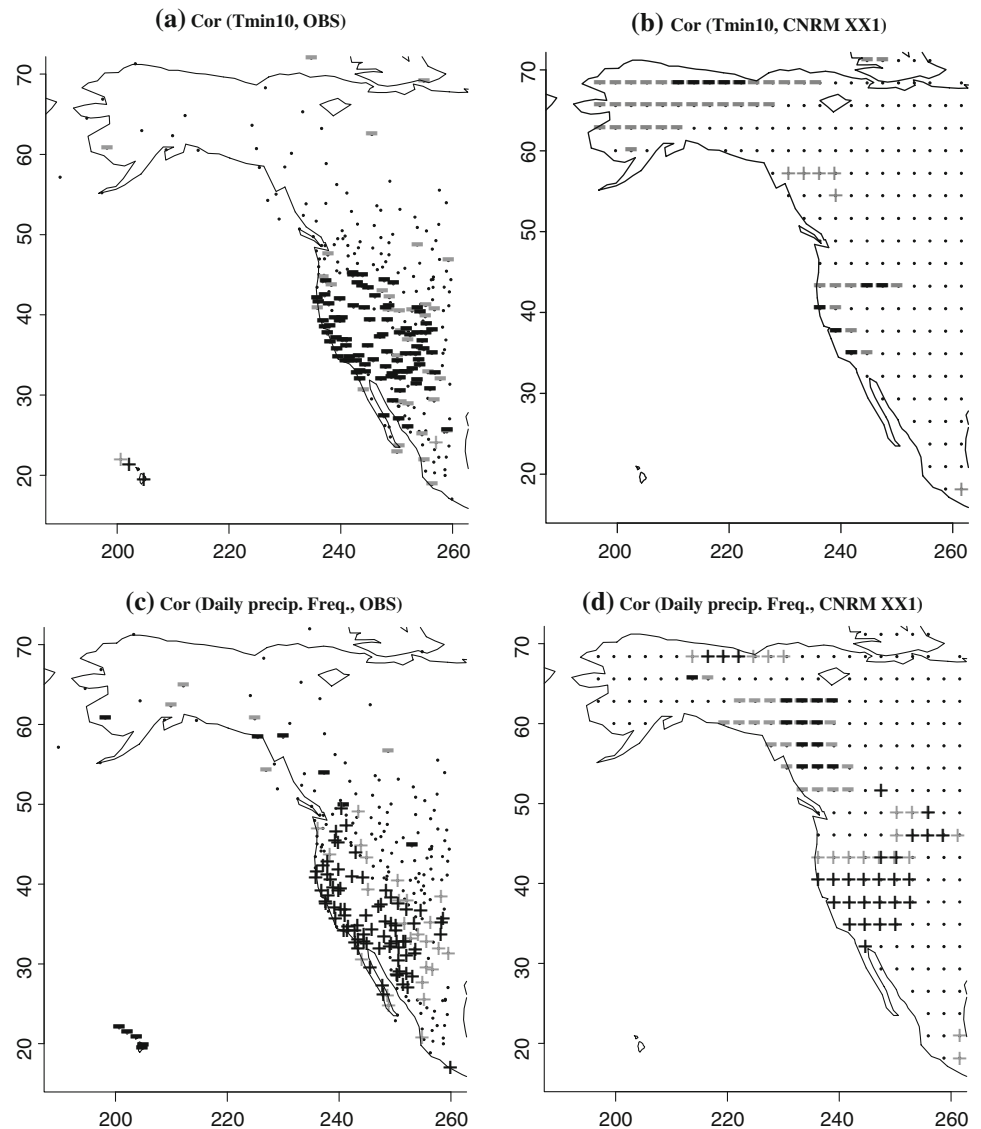


observed connection between the CF index and the tropical Pacific warm pool MSLP. Teleconnections with temperature and wind over the globe are weaker but also well reproduced in the model (Fig. 10c, d). Furthermore, when transient cyclones are more numerous in the study region (30° – 50° N/ 160° – 110° W), transient anticyclones are less frequent in this same northeast Pacific area ($r = -0.7$, sig. >99%, in the model and observations), see Fig. 12 and discussion of regional anticyclonic circulation below. Thus, when regional CF is high, regional MSLP (Fig. 10a, b) is low and a cyclonic low-level wind anomaly is centered off the continent (Fig. 10c, d). This mean configuration induces, in observations, and to a somewhat lesser extent in the model, colder temperatures over the central North Pacific and warmer conditions along the coast (Fig. 11) as well as over north western Mexico and over the western United States with less frequent extreme cold temperatures (Fig. 11a, b). Southerly wind anomalies along the coast favor heat and moisture transport from the eastern North Pacific tropical latitudes, and precipitation, which is more frequent during high CF index winters from northwestern Mexico to the Pacific Northwest (Fig. 11c, d). Further north, northeasterly wind anomalies advect continental air, reducing precipitation frequency over Alaska and British Columbia. In the model, patterns of extreme cold temperature and daily precipitation frequency are correctly reproduced, but the reduction/increase of cold extremes, when CF is positive/negative, is under-estimated over the West. Moreover, negative correlations appear over

Alaska in the model but no significant relation is found there in observations. As far as daily precipitation frequency (Fig. 11c, d), the model correctly reproduces the observed north–south correlation dipole. However, the north west of Mexico, as well as the states of Arizona and New Mexico do not present positive relation with CF in the model contrary to observations. Aside from these details, the model seems to be capable to reproduce the regional relationships between cyclonic frequency and weather. And since it also reproduces the main patterns of teleconnections between regional CF and basin-wide seasonally averaged climate, we can be confident in the model's ability to link regional weather over the West to global climatic influences and to do it for the right synoptic dynamical reasons.

The AF index (Fig. 12a, b), which summarizes regional anticyclone frequencies in the 40° N– 60° N/ 160° W– 120° W area, provides a dynamical link between the large-scale climate and the inter-annual variability of regional daily weather, for example, extreme cold temperature occurrences over the American Northwest (Fig. 14a, b). The positive phase of the AF index signifies anomalous regional anticyclonic activity from the Gulf of Alaska to the western United States (Fig. 12c, d). The negative phase reflects less frequent anticyclones along the West coast of North America and over the Aleutian region (Fig. 12e, f). The inter-annual variability of anticyclonic activity over the eastern North Pacific is correctly reproduced by the model in spite of a general underestimation of the frequency with

Fig. 11 Linear correlations between CF index and (a, b) extreme cold temperatures (frequency < to the tenth percentile) and (c, d) daily precipitation frequency. \pm = positive/negative correlation, grey = sig. >95%, black = sig. >99%. Left panels: observations, right panels: CNRM XX1. Daily precipitation frequency, from the CNRM model, has been computed considering only daily precipitation >1 mm



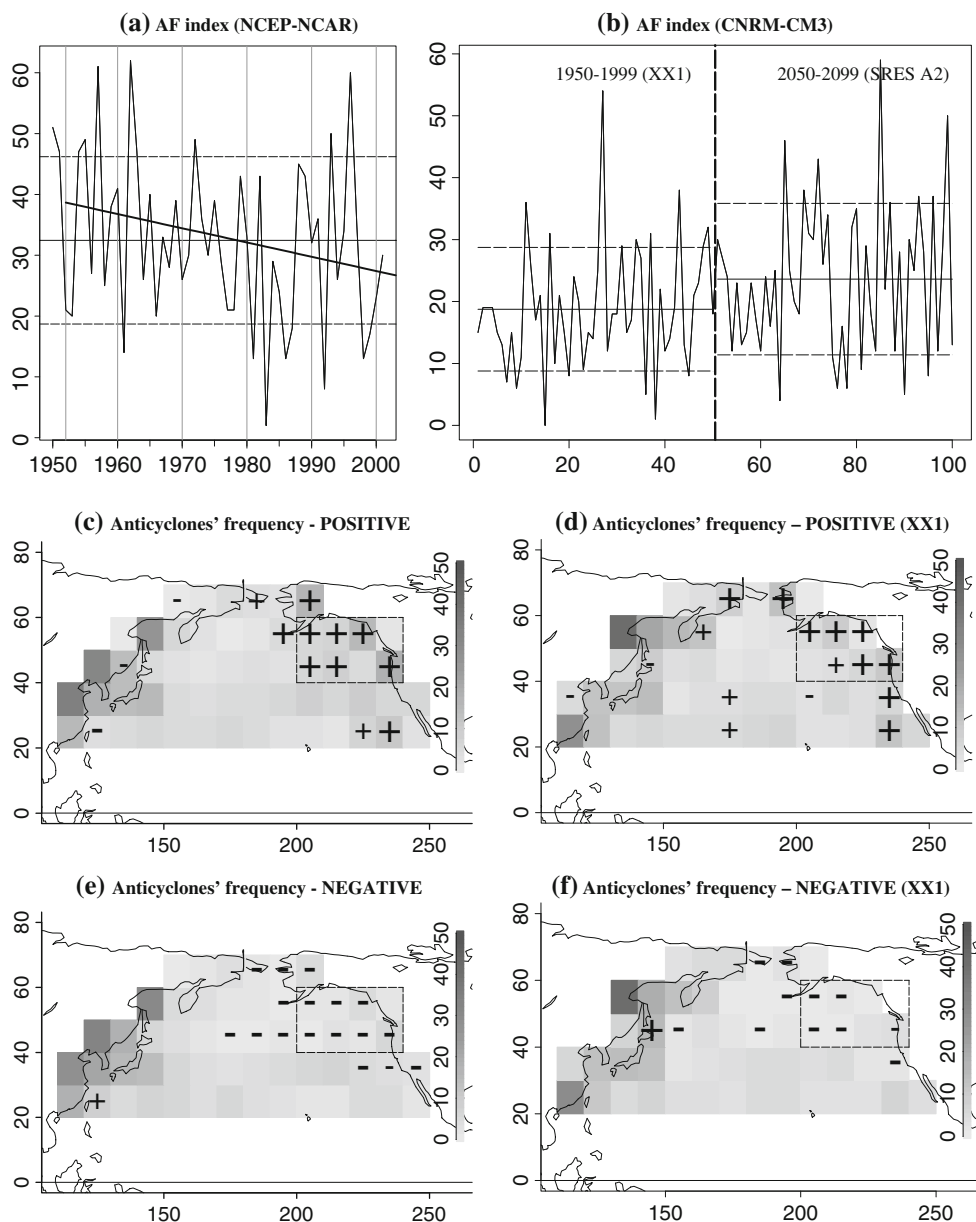
19 daily passages on average (standard deviation: 10) against 32 (standard deviation: 14) in reanalysis, averaged over the 40°N–60°N/160°W–120°W area.

Anticyclonic activity in the Gulf of Alaska and off British Columbia is negatively correlated with cyclonic activity in the same region (in reanalysis, $r = -0.6$, sig. >99%, and in the model, $r = -0.5$, sig. >99%). Thus, when transient anticyclones are more frequent, cyclones are less numerous inducing anomalously higher MSLP centered in the Gulf of Alaska (Fig. 13a, b). Higher MSLP there is associated with northern air advection along the coast and interior Canada favoring more frequent northerly outbreaks, which generate colder temperatures (Fig. 13c, d) and more frequent extreme cold events (Fig. 14a, b). When regional AF is high, precipitation frequency is significantly reduced over British Columbia while it is more frequently wet, probably via orographic uplift, on the east

side of the Rocky Mountains (Fig. 14c, d). The model correctly reproduces these features. Nevertheless, the model under-estimates impacts of transient anticyclones on extreme cold temperatures over California.

Over the North Pacific, when the AF index is positive, the anticyclonic circulation anomaly favors warmer temperatures over the central and western North Pacific including the Bering Sea. In the model, the structure of air temperature and wind anomalies is correctly reproduced but is not strong enough over the central and western North Pacific and, contrary to observations, no significant relation appears in the tropics. In observations, the pattern of temperature reveals an inverse relation between the AF index and inter-tropical temperatures (with NINO1.2, $r = -0.4$, sig. >95%). The model does not reproduce relationships between the AF index and inter-tropical climatic conditions in the Pacific Basin, for near-surface

Fig. 12 The AF index is computed summarizing daily occurrences of transient anticyclones in the area delimited on (c, d, e, f) from reanalysis (a) and (b) from the model historical simulation (XX1: from 1 to 50) and the SRES-A2 simulation (SRES A2: from 51 to 100). *Solid and dashed horizontal lines* represent means and standard deviation intervals, respectively, and *bolded line* the linear trend (reanalysis: -2.3 per decade, sig. $>95\%$). Positive composite (c, d) and negative composite (e, f) constructed from AF index (standard deviation method). *Shading*: anticyclones frequency; *signs \pm* : difference with mean field, sig. $>90\%$ and *bold signs* = sig. $>95\%$ (bootstrap test 1,000 samples chosen at random)

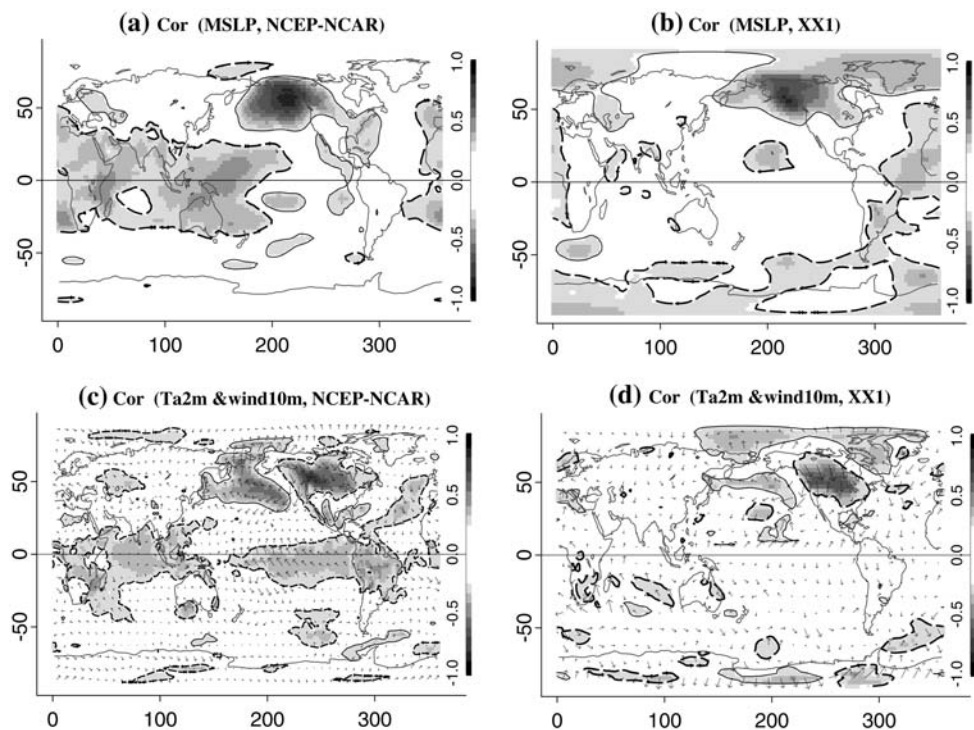


temperature as well as for wind and MSLP. A similar remark could be made for modeled cyclonic activity. In observations, cyclones' frequency off the US west coast (CF index) varies significantly with inter-tropical Pacific climate conditions, but the model is deficient in this regard (Fig. 10). Warmer temperatures in the inter-tropical zone (i.e., El Niño) favor cyclonic activity off the US west coast (correlation with NINO3.4 = 0.45, sig. $>95\%$ in reanalysis, 0.27, sig. = 95% in the model). Lambert (1996) and Lambert et al. (2002) have remarked that many models have difficulties to simulate links between strong mid-latitude cyclone occurrences and inter-tropical atmospheric conditions. This criticism applies to the CNRM-CM3, which underestimates the strength of the tropical

teleconnection to eastern North Pacific cyclonic activity (CF) and more generally in the North Pacific Basin.

In the model, the MSLP patterns associated with NINO3.4 and PDO are not strong enough over the Pacific Basin (not shown). Consequently, the AL index is poorly correlated with NINO 3.4 (-0.15 , not significant in the model compared to -0.43 , sig. $>99\%$, in reanalysis) and with PDO (-0.30 , sig. $>95\%$ in the model compared to -0.73 , sig. $>99\%$, in reanalysis). An important point is that the model does not reproduce the dipole between the AL and the western tropical Pacific MSLP. The features of this dipole (strength and coverage) determine the wind patterns in the North Pacific and in the inter-tropical convergence zone. This deficiency is equally associated with

Fig. 13 Linear correlations between AF index and MSLP (a, b), Ta2 m and wind10 m (c, d). Shading = significant correlation (>95%), *continue lines* = positive values, *dashed lines* = negative values. *Left panels*: NCEP-NCAR, *right panels*: CNRM XX1



an absence of the SPCZ (South Pacific Convergence Zone) in the model. The general underestimation of the relationships between SSTs and MSLP anomalies logically extends to transient activity, which is poorly correlated with SST anomalies in the model.

In this section, it was shown that synoptic transient frequency variations explaining precipitation and frequencies of cold outbreaks over western North America are generally linked with seasonal mean climate conditions in the Pacific Basin with clear connections to the AL, extratropical SSTs, as well as ENSO. The model correctly reproduces most of these features except for ENSO teleconnections, which are underestimated in the case of eastern North Pacific cyclonic activity and not reproduced at all in the case of anticyclones.

5.2 Projected impacts on the western North American climate

To understand the possible impacts of global warming on western North American climate, we have derived the regional cyclonic (CF) and anticyclonic (AF) indices presented in Sect. 5.1 in the SRES A2 projection (Figs. 9b, 12b). According to the model projection for the second half of the century, cyclone frequencies and the inter-annual variability tend to be reduced (difference between SRES A2 and XX1 = -6.34 for the mean, t -test sig. >99% and -3.7 for standard deviation, F -test sig. >99%) in the mid-latitude Northeastern Pacific (Fig. 9b). The general decline

of cyclones could diminish precipitation frequencies to the South of $\sim 40^\circ\text{N}$ (Fig. 15b). However, the pole-ward displacement of cyclone trajectories would increase daily precipitation frequency north of 45°N and most strongly over Alaska.

Polar outbreaks, associated with anticyclone incursions are projected to become more frequent (difference between SRES A2 and XX1 = $+4.9$ for the mean, t -test sig. >95% and no significant difference for the variance) over the Northeastern Pacific (Fig. 12b), which would reduce warming along the coast. In the SRES A2 simulation, frequency of cold outbreaks reduced all over Western North America but less strongly over regions affected by more frequent transient anticyclones, for example, southern Alaska, southwestern Canada, especially British Columbia, and along the West Coast of the United-States (Fig. 15a).

To synthesize, under advanced global warming in this GCM and most others (e.g., Koenig et al. 1993; Lambert 1995; Lunkeit et al. 1998; Sewall and Sloan 2004; Sewall 2005; Lambert and Fyfe 2006), cyclones are projected to move further to the north and for the North Pacific Basin, mean cyclonic activity is displaced westward toward Asia. The northwestward displacement of cyclone frequency should be more favorable to the formation and/or propagation of anticyclones over the central and eastern Pacific. These mean characteristics could contribute to restraining the warming along the west coast of North America and reducing precipitation frequency over the Southwestern

Fig. 14 Linear correlations between AF index and (a, b) extreme cold temperatures (frequency < to the tenth percentile) and (c, d) daily precipitation frequency. \pm = positive/negative correlation, grey = sig. >95%, black = sig. >99%. Left panels: observations, right panels: CNRM XX1. Daily precipitation frequency, from the CNRM model, has been computed considering only daily precipitation >1 mm

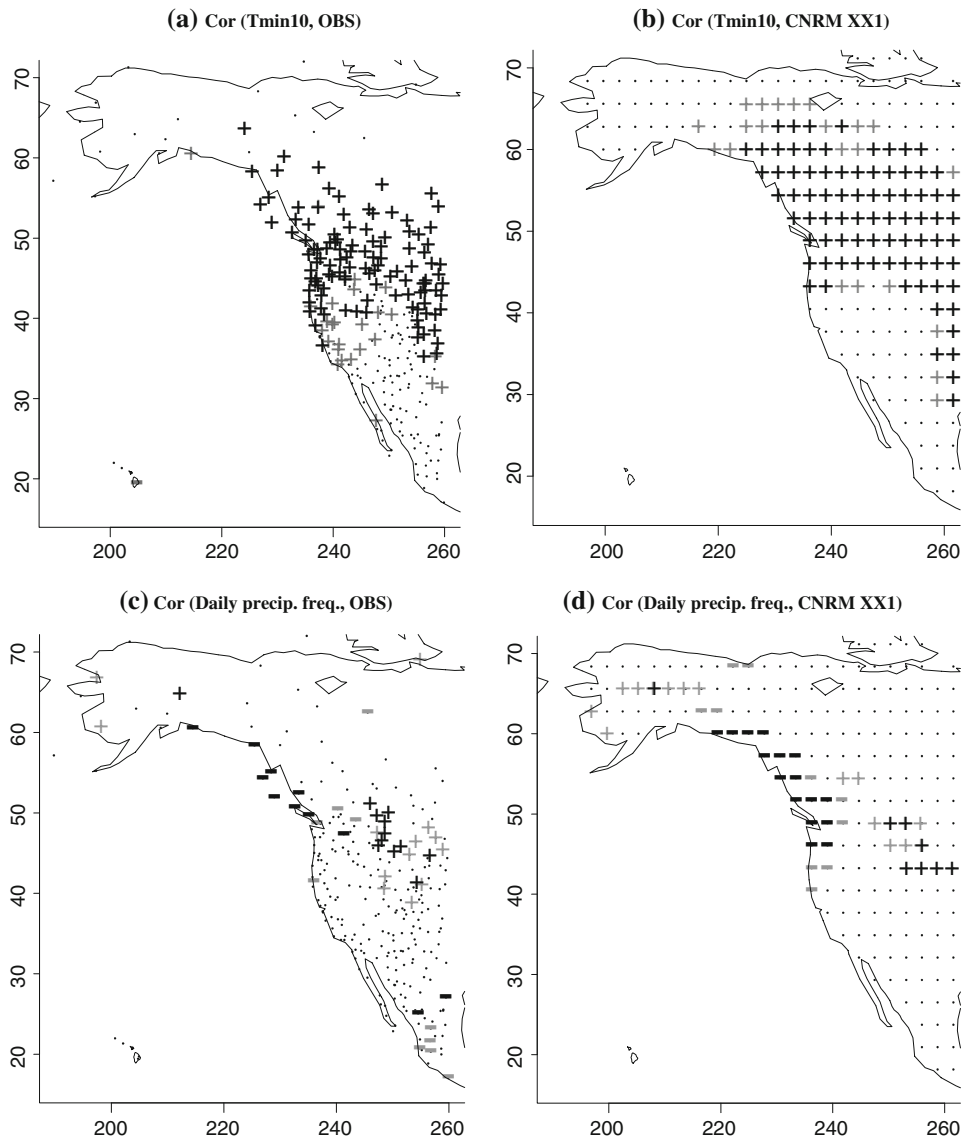
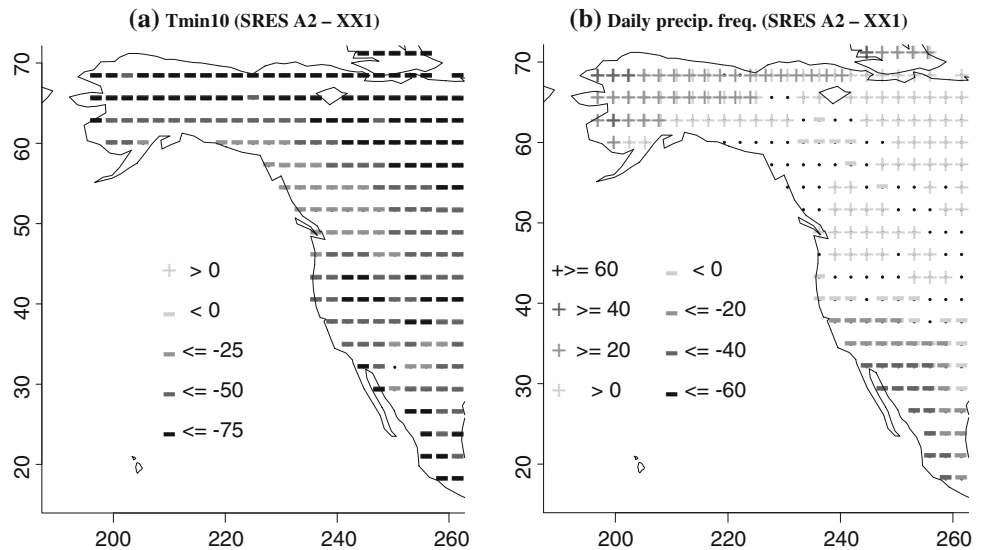


Fig. 15 Difference, expressed in percentage, between SRES A2 and historical simulations for extreme cold temperatures' frequency (a), and daily precipitation frequency (on the base of the full period 1950–2099, *t*-test: signs \pm = sig. >95%) (b). Daily precipitation frequency, from the CNRM model, has been computed considering only daily precipitation >1 mm



United States. They could, at the same time, favor precipitation further to the North.

6 Summary and conclusions

In spite of an overestimation of MSLP inducing a general underestimation of cyclone frequencies in the mid-latitude North Pacific, the modeled historical simulation correctly reproduces the spatial distribution of general cyclonic and anticyclonic features: the trajectories and mean structure of frequency. Although the model is able to reproduce most large-scale teleconnections to North Pacific transient activity, modeled teleconnections to tropical climate are severely underestimated. The model is also able to reproduce the general features of regional transient effects on intra-seasonal temperature and precipitation statistics.

Under advanced global warming, the model predicts a reduction of cyclones over the mid-latitude North Pacific and more frequent cyclones along the Asian coast from the Okhotsk Sea to the Bering Strait. The mid-latitude transient high response is more localized with fewer systems projected along the Asian coast, over the western Bering Sea and in the Gulf of Alaska, and more systems from the central North Pacific to the United States coast.

In general, warmer temperatures over the continents, especially at higher latitudes where warming is enhanced by melting ice as observed and further projected by models in the Northern Hemisphere would generate, as previous studies have suggested, a decreased equator-to-pole thermal gradient and land-ocean thermal contrast. This should be unfavorable to cyclonic activity over the mid-latitude central and eastern North Pacific, an intuitive result borne out by model projections. In this scenario, cyclones are gradually more confined to the high latitudes and over the west side of the North Pacific, where baroclinic wave activity could be stronger, due to pronounced horizontal surface temperature differences. Projected winter circulation is generally displaced to the North, that is, the subtropical high retracts pole-ward (IPCC 2007) while the temperate circulation retreats. In the western North Pacific, the accentuated cyclonic activity could reinforce the equator-to-pole heat transport inducing a more pronounced warming and more rainfall. On the other hand, over the eastern North Pacific, cyclones are projected to be confined further to the North, favoring more frequent anticyclones, which can moderate the warming over western North America and result in less frequent precipitation to the south of approximately 40°N. This possibility is consistent with results of Sewall (2005), who predict a decrease (increase) of precipitation over the southwestern (northwestern) North America in response to a general decline of the Arctic sea ice cover. Models also predict a general

increase of moisture, which could regionally enhance deep cyclones and influence precipitation intensity (Lambert 1995; Lambert and Fyfe 2006).

Around 1976–1977, the North Pacific region has experienced a deep climatic modification, which was characterized by intensification and weakening of cyclonic and anticyclonic activity, respectively, in the Northeastern Pacific (FG2006). This shift in the mid-latitude atmospheric circulation has contributed to warming over western North America (e.g., Karl et al. 1984, 1986, 1993; Easterling 2002; Groisman et al. 2004) and more frequent intense precipitation over the southwestern United States (Gershunov and Cayan 2003). These observed circulation changes over the North Pacific run counter to those observed over the global midlatitudes, and also to changes projected by most models including CNRM-CM3, as well as to physical intuition about synoptic changes to expect from greenhouse warming. We therefore conclude that the mid-1970s North Pacific climate shift, although it contributed to the observed winter warming of the West, was a result of natural NPO/PDO variability that happened to temporarily suspend most of the other regional weather and climate modifications expected from anthropogenic climate change. This situation has apparently abated since the end of the observational period considered in this study and as evidenced by a largely non-descript NPO/PDO phase and predominantly dry conditions observed in the southwest US so far in the beginning of the twenty first century. Based on results presented here, we expect dry (wet) conditions to develop further in the southwest (northwest) and punctuated with frequent cold outbreaks along the west coast of North America moderating the general warming. These changes are expected to develop in parallel with natural decadal and inter-annual variability that will sometimes mask and sometimes intensify certain aspects of the projected regional trends over the coming decades. In any case, explicit consideration of synoptic circulation anomalies is paramount to understanding observed and projected regional weather and climate changes in the mid-latitudes.

The synoptic approach affords a dynamical explanation for regional features of global climate change consistently predicted by models. This perspective results in a more accurate and detailed conceptual knowledge of likely regional future climate evolution. Results presented in this study need to be verified and better understood in future work including additional models and scenarios. It would also be useful to examine other world regions such the North Atlantic, Europe, and Asia. The synoptic approach can also form the basis of regional climate change downscaling and validation to be pursued in future work.

Acknowledgments We thank Mary Tyree and Sophie Tyteca for help with data processing. We are grateful to Hervé Douville for

providing invaluable comments on the original version of the manuscript. We also thank two anonymous reviewers for their constructive comments. Partial funding was provided by California Climate Change Center, sponsored by the California Energy Commission's Public Interest Energy Research Program and by the NOAA Office of Global Programs, under the California Applications Program. This work was also partially supported through NSF grant ATM-0236898. Results of this study contribute to the NATO Science for Peace project (SFP 981044) as well as the UC MEXUS-CONACYT program.

References

- Anderson JR, Gyakum JR (1989) A diagnostic study of Pacific Basin circulation regimes as determined from extratropical cyclone tracks. *Mon Weather Rev* 117:2672–2686
- Barnston AG, Livezey RE (1987) Classification, seasonality, and persistence of low-frequency atmospheric circulation patterns. *Mon Weather Rev* 115:1083–1126
- Chapelon N, Douville H, Kosuth P, Oki T (2002) Off-line simulation of the Amazon water balance: a sensitivity study with implications for GSWP. *Clim Dyn* 19:141–154
- Déqué M, Braum A, Piedelievre JP, Marquet P, Daudin P, Guérémy JF, Geleyn JF, Bazile E, Piriou JM, Yessad K, Courtier P, Rochas P (1999) ARPEGE version 3, documentation algorithmique et mode d'emploi (in French, available from CNRM/GMGE, Météo-France, 42 avenue G. Coriolis, 31057 Toulouse, France)
- Dettinger M, Remond K, Cayan DR (2004) Winter orographic precipitation ratios in the Sierra Nevada-Large-scale atmospheric circulations and hydrologic consequences. *J Hydrometeor* 5:1102–1116
- Douville H, Royer JF, Mahfouf JF (1995a) A new snow parametrization for the Météo-France climate model Part I: Validation in stand-alone experiments. *Clim Dyn* 12:21–35
- Douville H, Royer JF, Mahfouf JF (1995b) A new snow parametrization for the Météo-France climate model. Part II: Validation in a 3-D GCM experiments. *Clim Dyn* 12:37–52
- Easterling DR (2002) Recent changes in frost days and the frost-free season in the United States. *Bull Am Meteor Soc* 83:1327–1332
- Favre A, Gershunov A (2006) Extra-tropical cyclonic/anticyclonic activity in North-Eastern Pacific and air temperature extremes in Western North America. *Clim Dyn* 26:617–629
- Geng Q, Sugi M (2003) Possible change of extratropical cyclone activity due to enhanced greenhouse gases and sulfate aerosols—Study with a high resolution AGCM. *J Clim* 16:2262–2274
- Gershunov A, Cayan D (2003) Heavy daily precipitation frequency over the contiguous United States: Sources of climatic variability and seasonal predictability. *J Clim* 16:2752–2765
- Gibelin AL, Déqué M (2003) Anthropogenic climate change over the Mediterranean region simulated by a global variable resolution model. *Clim Dyn* 18:225–240
- Graham NE, Diaz HF (2001) Evidence for intensification of North Pacific winter cyclones since 1948. *Bull Am Meteor Soc* 82:1869–1992
- Groisman PY, Knight RW, Karl TR, Easterling DR, Sun B, Lawrimore JM (2004) Contemporary changes of the hydrological cycle over the contiguous United States: trends derived from in-situ observations. *J Hydrometeor* 5:64–85
- Gulev SK, Zolina O, Grigoriev S (2001) Extratropical cyclone variability in the Northern Hemisphere winter from the NCEP/NCAR reanalysis data. *Clim Dyn* 17:795–809
- Gyakum JR, Anderson JR, Grumm RH, Gruner EL (1989) North Pacific cold-season surface cyclone activity. *Mon Weather Rev* 117:1141–1155
- Hanson HP, Long B (1985) Climatology of cyclogenesis over the East China Sea. *Mon Weather Rev* 113:697–707
- Holland MM, Bitz CM (2003) Polar amplification of climate change in coupled models. *Clim Dyn* 21:221–232
- IPCC (2007) Working Group I, Climate Change 2007: The Physical Science basis
- Jhun JG, Lee EJ (2004) A new East Asian winter monsoon index and associated characteristics of the winter monsoon. *J Clim* 17:711–726
- Kalnay E, Kanamitsu M, Kistler R, Collins W, Deaven D, Gandin L, Iredell M, Saha S, White G, Woollen J, Zhu Y, Leetmaa A, Reynolds B, Chelliah M, Ebisuzaki W, Higgins W, Janowiak J, Mo KC, Ropelewski C, Wang J, Jenne R, Joseph D (1996) The NCEP/NCAR 40-year reanalysis project. *Bull Am Meteor Soc* 77:437–471
- Karl TR, Kukla G, Gavin J (1984) Decreasing diurnal temperature range in the United States and Canada from 1941 through 1980. *J Applied Meteor* 23:1489–1504
- Karl TR, Kukla G, Gavin J (1986) Relationship between decreased temperature range and precipitation trends in the United States and Canada, 1941–80. *J Applied Meteor* 25:1878–1886
- Karl TR, Jones PD, Knight RW, Kukla G, Plummer N, Razuvayev V, Gallo KP, Lindsey J, Charlson RJ, Petersen TC (1993) A new perspective on recent global warming: asymmetric trends of daily maximum and minimum temperature. *Bull Am Meteor Soc* 74:1007–1023
- Koenig WR, Sausen R, Sielmann F (1993) Objective identification of cyclones in GCM simulations. *J Clim* 6:2217–2231
- Kistler R, Kalnay E, Collins W, Saha S, White G, Woollen J, Chelliah M, Ebisuzaki W, Kanamitsu M, Kousky V, van den Dool H, Jenne R, Fiorino M (2001) The NCEP-NCAR 50-year reanalysis: monthly means CD-ROM and documentation. *Bull Amer Meteor Soc* 82:247–267
- Klein WH (1957) Principal tracks and mean frequencies of cyclones and anticyclones in the Northern Hemisphere. Weather bureau research paper no.40, US Department of Commerce, NOAA, Washington, D.C., pp 60
- Lambert SJ (1995) The effect of enhanced greenhouse warming on winter cyclone frequencies and strengths. *J Clim* 8:1447–14452
- Lambert SJ (1996) Intense extratropical Northern Hemisphere winter cyclone events: 1899–1991. *J Geophys Res* 101:319–325
- Lambert SJ, Fyfe JC (2006) Changes in winter cyclone frequencies and strengths simulated in enhanced greenhouse warming experiments: results from the models participating in the IPCC diagnostic exercise. *Clim Dyn* 26:713–728
- Lambert SJ, Sheng J, Boyle J (2002) Winter cyclone frequencies in thirteen models participating in the Atmospheric Model Intercomparison Project (AMIP1). *Clim Dyn* 19:1–16
- Lunkeit F, Bauer SE, Fraedrich K (1998) Storm tracks in a warmer climate: sensitivity studies with a simplified global circulation model. *Clim Dyn* 14:813–826
- Madec G, Delecluse P, Imbard M, Lévy C (1998) OPA version 8.1 Ocean general circulation model reference manual, Notes du Pôle de Modélisation, Institut Pierre-Simon Laplace, no. 11, pp 91 [Available from Laboratoire d'Océanographie Dynamique et de Climatologie, Université Paris VI, Paris 75252, France]
- Mahfouf JF, Manzi A, Noilhan J, Giordani H, Déqué M (1995) The land surface scheme ISBA within the Météo-France climate model ARPEGE Part I: Implementation and preliminary results. *J Clim* 8:2039–2057
- McCabe GJ, Clark MP, Serreze MC (2001) Trends in Northern Hemisphere surface cyclone frequency and intensity. *J Clim* 14:2763–2768
- McLay JG, Martin JE (2002) Surface cyclolysis in the North Pacific Ocean Part III: Composite local energetics of tropospheric-deep

- cyclone decay associated with rapid surface cyclolysis. *Mon Wea Rev* 130:2507–2529
- Mantua NJ, Hare SR, Zhang Y, Wallace JM, Francis RC (1997) A Pacific interdecadal climate oscillation with impacts on salmon production. *Bull Amer Meteor Soc* 78:1069–1079
- Martin JE, Grauman RD, Marsili N (2001) Surface cyclolysis in the North Pacific Ocean Part I: a synoptic climatology. *Mon Wea Rev* 129:748–765
- Miranda S (2003) Actualizacion de la base de datos ERIC II. Final report of the project TH-0226, IMTA internal reports
- NCDC (2003) Data documentation for data set 3200 (DSI-3200) Surface land daily cooperative summary of the day. National Climatic Data Center, Asheville, NC, p 36 [www.ncdc.noaa.gov/pub/data/documentlibrary/tddoc/td3200.pdf.]
- Noilhan J, Planton S (1989) A simple parameterization of land surface processes for meteorological models. *Mon Wea Rev* 117:536–549
- Oki T, Sud YC (1998) Design of Total Runoff Intergrating Pathways (TRIP) A global river channel network. *Earth Interactions*, vol. 2. paper 1
- Ovland JE, Adams JM, Bond NA (1999) Decadal variability of the Aleutian Low and its relation to high-latitude circulation. *J Clim* 12:1542–1548
- Panagiotopoulos F, Shahgedanova M, Hannachi A, Stephenson DB (2005) Observed trends and teleconnections of Siberian High: a recently declining center of action. *J Clim* 18:1411–1422
- Pettersen S (1956) *Weather analysis and forecasting*, vol. 1. McGraw-Hill, pp 422
- Pezza AB, Ambrizzi T (2003) variability of Southern Hemisphere cyclone and anticyclone behavior: further analysis. *J Clim* 16:1075–1083
- Ralph FM, Neiman PJ, Rotunno R (2004) Dropsonde observations in low-level jets over the Northeastern Pacific Ocean from CALJET-1998 and PACJET-2001: mean vertical-profile and atmospheric-river characteristics. *Mon Wea Rev* 133:889–910
- Reed RJ, Albright (1986) A case study of explosive cyclogenesis in the eastern Pacific. *Mon Wea Rev* 114: 2297–2319
- Roebber PJ (1984) Statistical analysis and updated climatology of explosive cyclones. *Mon Wea Rev* 112:1577–1589
- Roebber PJ (1989) On the statistical analysis of cyclone deepening rates. *Mon Wea Rev* 117:2293–2298
- Rogers E, Bosart LF (1986) An investigation of explosively deepening oceanic cyclones. *Mon Wea Rev* 114:702–718
- Salas Mélia D (2002) A global coupled sea ice-ocean model. *Ocean Model* 4:137–172
- Salas-Mélia D, Chauvin F, Déqué M, Douville H, Guérémy JF, Marquet P, Planton S, Royer JF, Tyteca S (2005) Description and validation of the CNRM-CM3 global coupled model, CNRM working note 103
- Sanders F, Gyakum JR (1980) Synoptic-dynamic climatology of the “bomb”. *Mon Wea Rev* 108:1589–1606
- Serreze MC, Carse F, Barry RG, Rogers JC (1997) Icelandic low cyclone activity: climatological features, linkages with the NAO, and relationships with the recent changes in the northern hemisphere circulation. *J Clim* 10:453–464
- Sewall JO (2005) Precipitation shifts over western North America as a result of declining Arctic sea ice cover: The coupled system response. *Earth Interactions* 9:1–23
- Sewall JO, Sloan LC (2004) Disappearing Arctic sea ice reduces available water in the American west. *Geophys Res Lett* 31:L06209. doi:10.1029/2003GL019133
- Simmonds I, Keay K (2000a) Mean Southern Hemisphere extra-tropical cyclone behavior in the 40-year NCEP-NCAR reanalysis. *J Clim* 13:873–885
- Simmonds I, Keay K (2000b) Variability of Southern Hemisphere extra-tropical cyclone behaviour, 1958–1997. *J Clim* 13:550–561
- Trenberth KE (1990) Recent observed interdecadal climate changes in the Northern Hemisphere. *Bull Amer Meteor Soc* 71:988–993
- Trenberth KE, Hurrell JW (1994) Decadal atmosphere-ocean variations in the Pacific. *Clim Dyn* 9:303–319
- Vincent LA, Gullett DW (1999) Canadian historical and homogeneous temperature datasets for climate change analyses. *Int J of Clim* 19:1375–1388
- Wallace JM, Gutzler DS (1981) Teleconnections in the geopotential height field during the Northern Hemisphere winter. *Mon Weather Rev* 109:748–812
- Wallace JM, Lim GH, Blackmon (1988) Relationship between cyclone tracks, anticyclone tracks, and baroclinic waveguides. *J Atmos Sci* 45: 439–462
- Yin JH (2005) A consistent poleward shift of the storm tracks in simulation of 21st century climate. *Geophys Res Lett* 32:L18701. doi: 10.1029/2005GL023684
- Zhang Y, Wang WC (1997) Model-simulated northern winter cyclone and anticyclone activity under a greenhouse warming scenario. *J Clim* 10:1616–1636
- Zhu X, Sun J, Liu Z, Liu Q, Martin JE (2007) A synoptic analysis of the interannual variability of winter cyclone activity in the Aleutian Low region. *J Clim* 20:1523–1538
- Zolina O, Gulev SK (2002) Improving the accuracy of mapping cyclone numbers and frequencies. *Mon Weather Rev* 130:748–759